Synchrotron Radiation X-ray Diffraction Study on Phase Behavior of PPP–POP Binary Mixtures

A. Minato[a,*], S. Ueno[a], J. Yano[a], Z.H. Wang[b], H. Seto[c], Y. Amemiya[d], and K. Sato[a]

[a]Faculty of Applied Biological Science, Hiroshima University, Higashi-Hiroshima 739, Japan, [b]Hei Long Jiang Commercial College, People's Republic of China, [c]Faculty of Integrated Arts and Sciences, Hiroshima University, Higashi-Hiroshima 739, Japan, and [d]National Laboratory for High-Energy Physics, Tsukuba 305, Japan

ABSTRACT: The phase behavior of the *sn*-1,3-dipalmitoyl-2-oleoylglycerol (PPP–POP) binary mixture system was studied by powder X-ray diffraction with synchrotron radiation and by differential scanning calorimetry. The results showed that the immiscible phases were observed in metastable and in the most stable forms. In particular, synchrotron X-ray diffraction enabled us to reveal the monotectic nature of α as a kinetic phase behavior. The equilibrium phase diagram of the PPP–POP mixture is divided into two regions. In POP concentration ratios below 40%, solid-state transformation from α to β was observed, indicating that the α-β transition of PPP was promoted in the presence of POP. By contrast, the polymorphic transition proceeds from α to β through the occurrence of the intermediate β′ form at POP concentration ratios above 50%.
JAOCS 73, 1567–1572 (1996).

KEY WORDS: Differential scanning calorimetry, mixture phase behavior, 2-oleodipalmitin, polymorphism, synchrotron radiation X-ray diffraction, tripalmitin.

Triacylglycerols (TAG) are main components of fat products and play dominant roles in structure–property relationships, in which polymorphism is of the highest importance. In pure systems, polymorphism of TAG has been elucidated at highly detailed levels compared to mixed systems (1).

As to the phase behavior of binary mixture systems, three typical phases can occur when the two components are miscible in a liquid state: solid solution, eutectic phase, and compound formation (2). Various types of phase diagrams of TAG mixtures have been reviewed by Rossell (3) and Small (4). For example, in the binary system of tripalmitoylglycerol–tristearoylglycerol (PPP–SSS), the metastable forms α and β′ exhibit continuous solid solution, yet the most stable form, β, is eutectic (5). A recent study of the PPP–SSS mixture at a 1:1 ratio by time-resolved synchrotron X-ray diffraction has revealed the dynamic aspect of the transformation in the mixed system, making it possible to follow the rapid crystallization and transformation at scanning rates of several degrees per minute (6–8). It has become evident that synchrotron radiation is the most powerful X-ray tool to study kinetic processes of polymorphism behavior. This technique also reinforced the results of differential scanning calorimetry (DSC) experiments.

For PPP–POP (*sn*-1,3-dipalmitoyl-2-oleoylglycerol) mixtures, Kerridge (9) reported that they exhibited a monotectic nature in the most stable form. Gibon *et al.* (10) also studied this system and claimed that the metastable forms of the mixture are partly miscible. At that time, polymorphism of POP had not been unveiled, especially in the metastable forms. Sato *et al.* (11,12) revealed the polymorphism of POP, SOS (*sn*-1,3-distealoyl-2-oleoyl-glycerol) and POS (*sn*-1,3-palmitoylstealoyl-2-oleoylglycerol), by means of highly purified samples.

The present study reports the structural aspects in the phase behavior of PPP–POP mixture by using highly purified samples and shows dynamical properties of the polymorphic behavior obtained from synchrotron X-ray radiation. A careful analysis has been done on the molecular interactions between POP and PPP present in this mixture based on their chainlength structure. The polymorphic behavior of PPP and POP is shown in Table 1 (11,13). The chainlength in the most

TABLE 1
Melting Points and XRD Long-Spacing of Polymorphs of POP (Ref. 11) and PPP (Ref. 13)[a]

	PPP			POP				
	α	β′	β	α	γ	β′	β2	β1
Melting point (°C)	44.7	56.6	66.4	15.2	27.0	30.3	35.1	36.7
Long spacing (nm)	4.60	4.23	4.09	4.65	6.54	4.24	6.13	6.05
Chainlength structure	Double	Double	Double	Double	Triple	Double	Triple	Triple

[a]PPP–POP, *sn*-1,3-dipalmitoyl-2-oleoylglycerol; XRD, X-ray diffraction.

*To whom correspondence should be addressed.

stable β-form of PPP is double, but that of the two β-forms of POP is triple. However, the double chainlength structure appeared in the metastable β′-forms of PPP and POP. Therefore, it is interesting to see how the chainlength structure is affected by mixing of POP and PPP in the β′-form during crystallization and transformation. The phase behavior of PPP–POP is related to food industrial applications, such as in the fractionation of palm oil, in which the interactions of PPP and POP seem important during the crystallization of palm olein at low temperatures.

EXPERIMENTAL PROCEDURES

Materials and methods. PPP and POP were purchased from Sigma Chemical Co. (St. Louis, MO) at 99% purity and used without further purification.

The mixtures were prepared by mixing and melting at 80°C, which was followed by rapid cooling below 5°C. Polymorphic forms were obtained by simple cooling and tempering. Identification of each polymorphic form was accomplished by powder X-ray diffraction [(XRD) Cu-Kα, 30kV and 10mA; Rigaku, Tokyo, Japan] measurements of a traditional type. Thermal measurements were performed with a Rigaku DSC-8230 by heating at a rate of 2°C/min and with a DSC-50 (Shimadzu, Kyoto, Japan) by cooling at a rate of 15°C/min. The synchrotron radiation XRD (SR–XRD) experiments were carried out with a Photon Factory (PF), a synchrotron radiation source at the National Laboratory for High-Energy Physics (Tsukuba, Japan). PF is operating at 2.5 GeV. The XRD patterns were recorded every 10 s with a gas-filled one-dimensional position-sensitive detector (512 channels over a total length of 20 cm, Rigaku). For the wide-angle XRD measurements, the distance between the sample and the X-ray beam detector was 280 mm. The temperature was controlled by two water baths and recorded in combination with the XRD data. The time-resolved XRD was measured during rapid cooling and heating processes.

The thermodynamically most stable forms were obtained by two-stage thermal incubations: the mixture liquid was quenched at 0°C to crystallize the whole sample. Then, temperature was raised to 40°C, which is far above the melting point of the most stable form of POP. At 40°C, incubation was carried out over 7 d to attain stabilization for PPP. Thereafter, the sample was cooled to 30°C, and incubation at this temperature was 7 d to attain stabilization for POP.

RESULTS AND DISCUSSION

Phase diagram of the PPP–POP binary mixture. Figure 1 shows the DSC heating thermograms of the most stable forms of three PPP–POP mixtures. The mixture of PPP/POP = 60:40 shows a single peak at 63°C, which corresponds to melting of β. The polymorphic form was confirmed by XRD. In the 50:50 mixture, two peaks were observed at 38 and 58°C. The former is due to melting of POP β as characterized by XRD. The latter is of PPP β melting. Lowering and broadening in the melting behavior of PPP β are caused by solubility effects of PPP due to the presence of liquid POP. The same pattern was observed for the PPP/POP 10:90 mixture. From these data, we constructed a phase diagram of the PPP and POP binary mixture, which exhibits the monotectic nature of the PPP and POP binary mixture (Fig. 2).

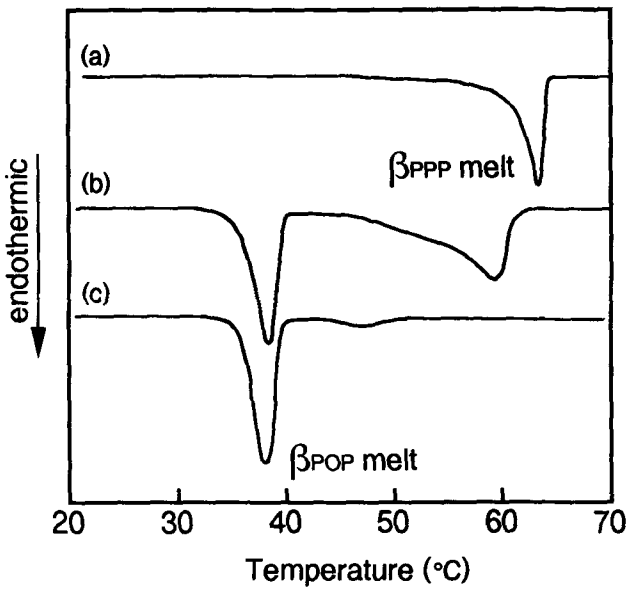

FIG. 1. Differential scanning calorimetry heating thermograms (2°C/min) of the most stable form of *sn*-1,3-dipalmitoyl-2-oleoylglycerol (PPP–POP) mixture. The ratios of PPP–POP are (a) 60:40, (b) 50:50, (c) 10:90.

One may compare Figure 2 with other binary mixtures of TAG, PPP–SSS (S = stearic), PPP–LLL (L = lauric) and SSS–LLL systems, in which the chainlength of the TAG differs by two, four and six carbons, respectively. A eutectic point

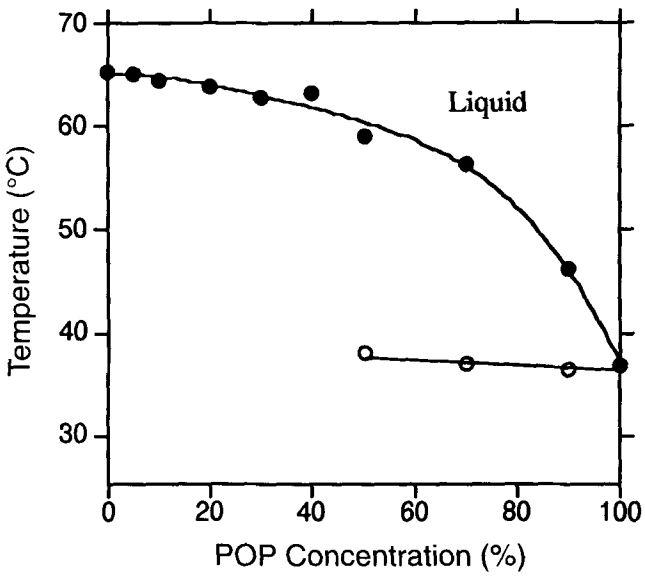

FIG. 2. Melting points of the most stable polymorphs of PPP–POP mixture; ● for PPP, ○ for POP. See Figure 1 for abbreviation.

is present at about 20% SSS concentration for the PPP–SSS mixtures (4,9). As the differences in the melting points of the component TAG increase, the eutectic phase tends to shift to a monotectic phase. For the PPP–LLL (9) and SSS–LLL systems (9), the phase diagrams demonstrate a monotectic phase. In these systems, the differences in the melting points between the high-melting and low-melting components are 18°C (PPP–LLL) and 28°C (SSS–LLL). Therefore, it is easy to understand that the PPP–POP mixture is monotectic because the melting point between the two components differs by 30°C. In addition, the difference in chainlength structure may be another factor in forming the immiscible nature; POP β2 has a triple strucure and PPP β is double.

The solubility of POP in PPP was about 40% in the most stable form. This result is in agreement with the phase diagram obtained by Kerridge (9) and with the intersolubility of β obtained by Gibon *et al.* (10).

A kinetic phase diagram. Figure 3A shows a DSC cooling thermogram of the POP 50% mixture, measured at a cooling rate of 15°C/min. Two exothermic peaks were observed at 36.2 and 14.6°C, which are crystallization temperatures of PPP α and POP α, respectively. The wide-angle XRD spectrum taken for this crystal was a single reflection at $2\theta = 21.4°$ (0.41 nm), which is characteristic of α. The XRD long spacing value was 4.6 nm, which also corresponds to the α-form of POP (11) and PPP (13). Figure 3B shows a kinetic phase diagram concerning the α-form of PPP and POP and demonstrates the monotectic type of α. The solubility of POP in the α-form of PPP is about 10%.

Concerning the phase behavior of intermediate β′-forms, Figure 4 was constructed by DSC heating measurements, in which the liquid mixtures were crystallized at 0°C and heated at a rate of 2°C/min. This kinetic phase diagram is divided into two regions at concentration ratios of PPP/POP between 60:40 and 50:50. In the PPP-rich region, the α-forms of both PPP and POP solidified below 20°C. Upon heating, both fractions transformed to the β-form. In the POP-rich region, however, the POP fraction revealed a successive α-β′-β transformation. The melting points of α- and β′-forms of PPP were not available above the POP 50% concentration. No DSC endothermic and exothermic peaks of PPP α- and β′-forms were observed, either because the metastable forms of PPP underwent solid-state transformation, or because they melted in the POP melting regions. Figure 5 displays typical DSC heating thermograms that relate to Figure 4. The polymorphic forms displayed in Figures 4 and 5 were confirmed by dynamic SR–XRD experiments as described in the following section.

Synchrotron radiation XRD spectra. Figure 6 shows a bird's-eye view of the short-spacing SR–XRD patterns of the PPP/POP = 90:10 mixture during the heating process from 9 to 67°C. When the mixture is cooled rapidly, the short-spacing pattern of 0.41 nm, specific to the hexagonal (H) subcell of PPP α and POP α, appeared. Then, upon heating, the short-spacing pattern changed to that characteristic of the β-form with the triclinic parallel ($T_{//}$) subcell. This change occurred at 40°C, which is identical to a small exothermic DSC peak

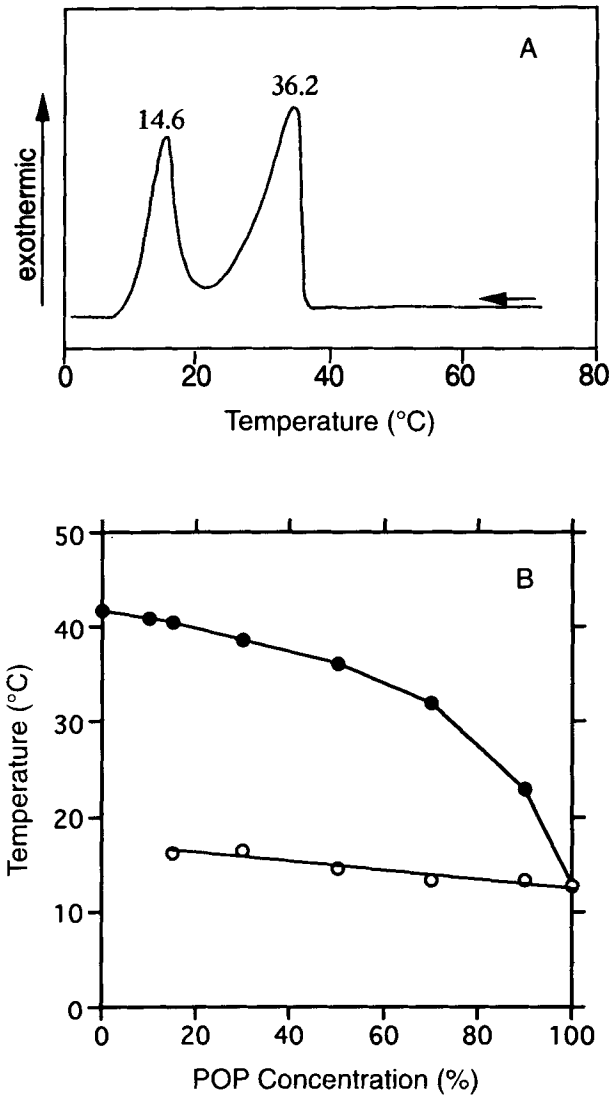

FIG. 3. (A) Differential scanning calorimetry cooling thermogram of PPP–POP (50:50) at a rate of 15°C/min. (B) A kinetic phase diagram of PPP–POP mixture. Exothermic peaks: ● for PPP, ○ for POP. See Figure 1 for abbreviation.

shown as an arrow in Figure 5B. It is clear that no β′-form occurred during the transformation from α to β.

Figure 7 shows the SR–XRD pattern of the PPP/POP = 50:50 mixture on heating from 13°C. The α-form first gradually transformed to β′ around 25°C and finally converted to β above 25°C. The α form was of PPP and POP. As for the β′-form, the first occurring fraction was of POP, which converts to β above 30°C, which is higher than the melting point of POP β′. The β′-form still present above 30°C was of PPP. The finally occurring β-form was of the PPP fraction. The corresponding DSC thermogram is shown in Figure 5C.

The SR–XRD measurements of POP 30% and POP 70% mixtures showed the same results as those of the POP 10% and POP 50% mixtures, respectively.

Figure 8 shows the SR–XRD spectra of the 50:50 blend of PPP/POP during the cooling process from 65 to 25°C, which

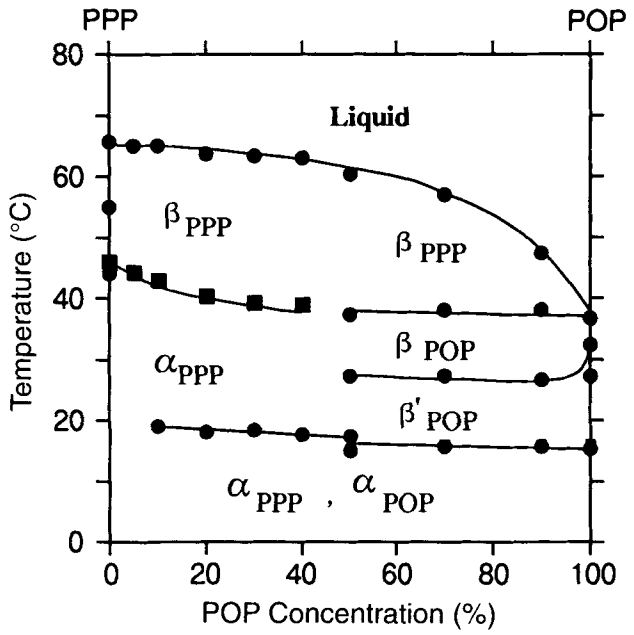

FIG. 4. A kinetic phase diagram of PPP–POP mixture constructed after differential scanning calorimetry measurements (2°C/min). ●, endothermic; ■, exothermic. See Figure 1 for abbreviation.

is far above the melting point of POP α. The crystallization of α of PPP was detectable at 38°C, and POP was crystallized in the β′-form soon after 25°C was reached. By contrast, when the sample was crystallized at 31°C (Fig. 9), the α-form of PPP crystallized around 41°C and rapidly started to transform to β during the cooling process at 31°C. As for the POP

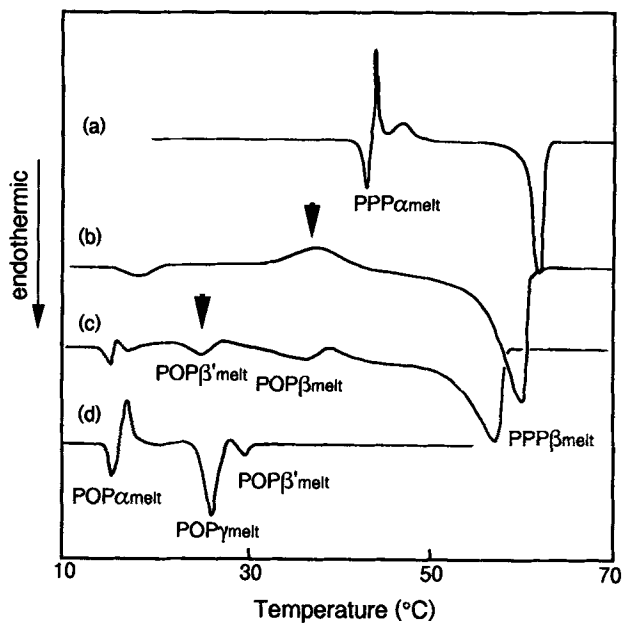

FIG. 5. Differential scanning calorimetry heating thermograms (2°C/min) of PPP–POP mixture. The ratio of PPP–POP are (a) 100:0, (b) 60:40, (c) 50:50, (d) 0:100. See Figure 1 for abbreviation.

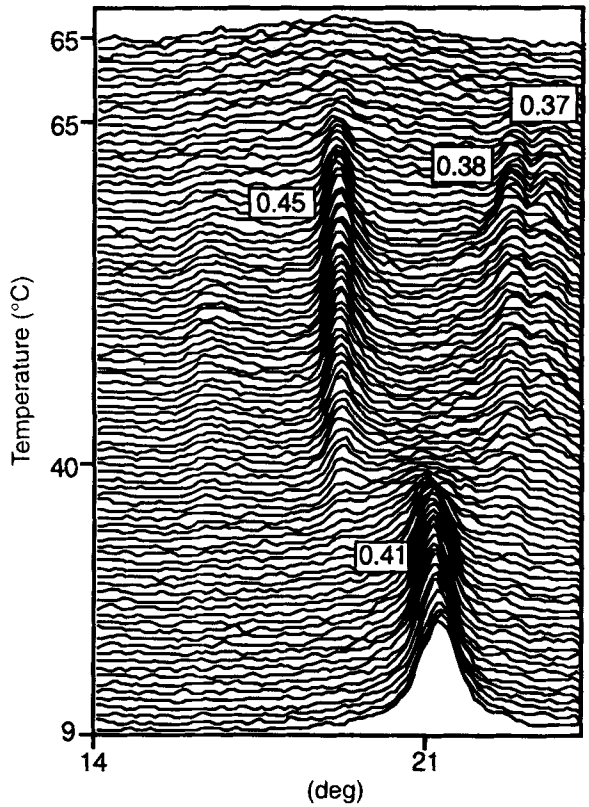

FIG. 6. Wide-angle synchrotron X-ray study of the α-β transition of a 90:10 mixture of PPP–POP. Units, nm. See Figure 1 for abbreviation.

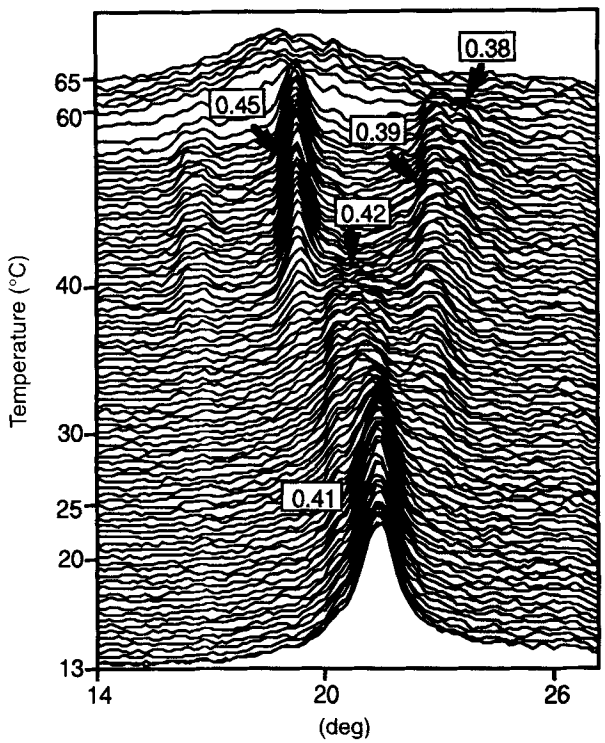

FIG. 7. Wide-angle synchrotron X-ray study of the transition of a 50:50 mixture of PPP–POP. Units, nm. See Figure 1 for abbreviation.

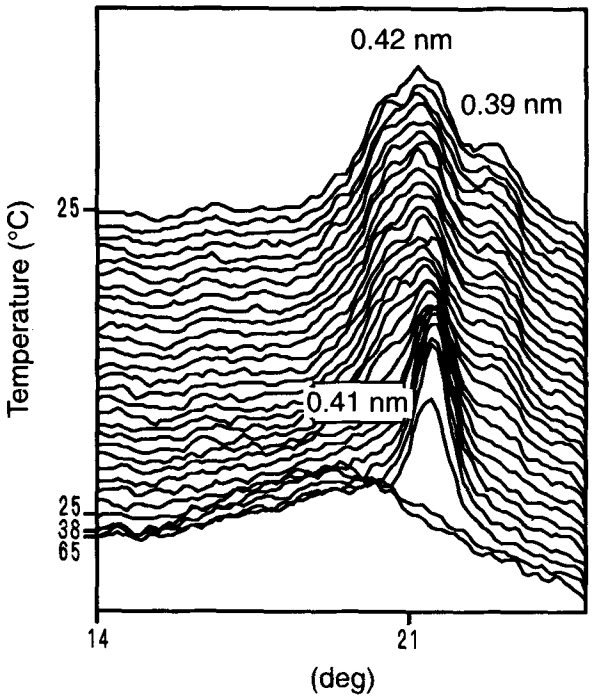

FIG. 8. Wide-angle synchrotron X-ray study of melt-β′ crystallization of a 50:50 mixture of PPP–POP at 25°C. See Figure 1 for abbreviation.

fraction, crystallization occurred in the β-form. No evidence is seen for β′ crystallization.

As for the transformation kinetics of PPP from α to β in the presence of POP, which is displayed by DSC in Figure 4, two interesting results were observed. In a range of POP concentration below 40%, PPP transformed from α to β with no passage through β′, which is accompanied with the exothermic heat of transformation. This behavior is in good contrast to the α–β transformation in pure PPP, which undergoes a melt-mediated conversion, sometimes through β′, as observed by SR–XRD (6,8). It is assumed that the exothermic α-β transformation of PPP, involving intersolubilized POP, may be caused by lattice instability of α, which enabled the conversion to β before the melting of itself.

By contrast, PPP transformed to β from α after stable occurrence of β′ in the POP concentration range above 50% (Figs. 4 and 7). This may be due to the effect of the presence of POP β′ in the monotectic phase. The molecular contacts between the PPP and POP crystal fractions might enable this polymorphic interaction. In the same concentration range, POP transformed from α to through β′ in the following manner. Below the melting point of POP β′ (30°C), β′ is rather stable. However, it converts to β above 30°C through β′-melt-mediated transformation (Fig. 5C, arrows), whose rate is quite high compared to the pure system. A similar result was observed in the PEP–POP (where E = elaidic) mixture (14), which showed that the presence of PEP in POP promotes the β′-β transformation of POP during melt-mediated crystallization.

The solubility of POP in PPP is apparently different between α and β. In α, the solubility is 10%, yet it is 40% for β. This may be due to a kinetic effect because a long incubation was carried out for β and quenching is only applied for α. If α would be incubated, the solubility might increase. But this process cannot be actually realized because the rapid transformation from α to more stable forms will occur.

Finally, in Figure 10, a time course of intensity of the diffraction peaks at its maximum is given during the crystallization and transition processes at the 10% POP concentration. We have taken 0.41 nm for α and 0.45 nm for β as references. The intensity of β increased after the intensity of α started to decrease on heating. It took about 250 s to completely transform from α to β in this mixture. This value is in good agreement with the DSC results (Fig. 5). The α-β transition could

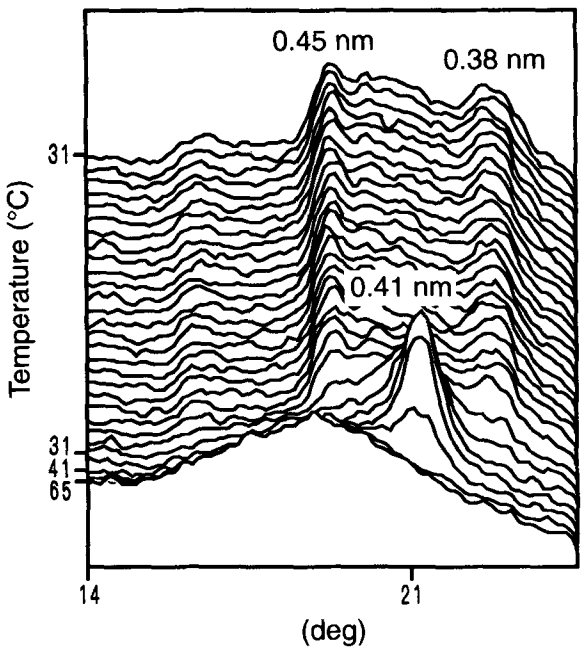

FIG. 9. Wide-angle synchrotron X-ray study of melt-β crystallization of 50:50 mixture of PPP–POP at 31°C. See Figure 1 for abbreviation.

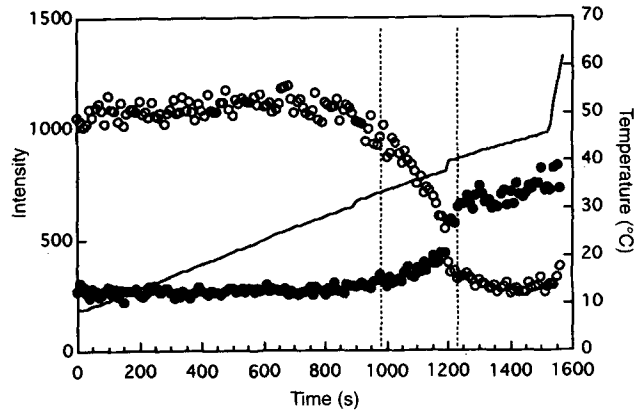

FIG. 10. Time variations of the maximum intensity of 19 and 21° (2θ) diffraction peaks corresponding to α-form and β-form, respectively, in the PPP–POP10% ; ○ for 4.6 nm, ● for 4.1 nm, and a solid line: temperature. See Figure 1 for abbreviation.

also be followed by observing the change in the d(001) spacing. Yet, the transition time was difficult to decide in this case, because the differences in the long spacing of α and β were too small to be detectable.

In the concentration ranges of POP above 50%, the polymorphic behavior was more complicated than that below 40% POP concentration as mentioned above. The crystallization or transition time of the mixture could not be obtained because it was difficult to differentiate the respective diffraction spectra. The maximum intensity was strongly influenced by crystal perfection and crystal size. Therefore, the measured intensities could not be used to determine the relative amounts of the different polymorphs.

To summarize, the PPP–POP binary system has shown immiscible monotectic properties in the metastable as well as in the stable forms. The polymorphic behavior of PPP–POP mixtures resulted in the following: (i) in the POP ratio below 40%, the α-β solid-state transformation of PPP was observed; (ii) in the POP ratio above 50%, the polymorphic transition proceeded from α to β through the intermediate β′ form, both for POP and PPP.

REFERENCES

1. Hagemann, J.W., in *Crystallization and Polymorphism of Fats and Fatty Acids,* edited by N.Garti and K. Sato, Marcel Dekker, New York, 1988, pp. 9–95.
2. Timms, R.E., Phase Behaviour of Fats and Their Mixtures, *Prog. Lipid. Res. 25*:1–38 (1984).
3. Rossell, J.B., Phase Diagrams of Triglyceride Systems, *Advance in Lipid Res. 5*:353–408 (1967).
4. Small, D.M., in The Physical Chemistry of Lipids, *Handbook of Lipid Research 4,* Plenum, New York, 1986, pp. 378–382.
5. Lutton, E.S., Phase Behavior of Triglyceride Mixture Involving Primarily Tristearin, 2-Oleyldistearin, and Triolein, *J. Am. Oil Chem. Soc. 32*:49–53 (1955).
6. Kellens, M., W. Meeussen, C. Riekel, and H. Reynaers, Time-Resolved X-ray Diffraction Studies of the Polymorphic Behaviour of Tripalmitin Using Synchrotron Radiation, *Chem. Phys. Lipids. 52*:79–98 (1990).
7. Kellens, M., W. Meeussen, A. Hammersley, and H. Reynaers, Synchrotron Radiation Investigation of the Polymorphic Transitions. Part 2: Polymorphism Study of 50:50 Mixture of Tripalmitin and Tristearin During Crystallization and Melting, *Ibid. 58*:145–158 (1991).
8. Kellens, M., W. Meeussen, R. Gehrke, and H. Reynaers, Synchrotron Radiation Investigations of the Polymorphic Transformations of Saturated Monoacid Triglycerides. Part 1: Tripalmitin and Tristearin, *Ibid. 58*:131–144 (1991).
9. Kerridge, R., Melting-Point Diagrams for Binary Triglyceride System, *J. Chem. Soc.,* 4577–4579 (1952).
10. Gibon, V., F. Durant, and Cl. Deroanre, Polymorphism and Intersolubility of Some Palmitic, Stearic and Oleic triglycerides: PPP, PSP and POP, *J. Am. Oil Chem. Soc. 63*:1047–1055 (1986).
11. Sato, K., T. Arishima, Z.h. Wang, K. Ojima, N. Sagi, and H. Mori, Polymorphism of POP and SOS. I. Occurrence and Polymorphic Transformation, *Ibid. 66*:664–674 (1989).
12. Yano, J., S. Ueno, K. Sato, T. Arishima, N. Sagi, F. Kaneko, and M. Kobayashi, FT-IR Study of Polymorphic Transformation in SOS, POP and POS, *J. Phys. Chem. 97*:12967–12973 (1993).
13. Lutton, E.S., and A.J. Fehl, The Polymorphism of Odd and Even Saturated Single Acid Triglycerides C8-C22, *Lipids 5*:91–99 (1969).
14. Lovegren, N.V., M.S. Gray, and R.O. Feuge, Thermal Properties of 2-Oleodipalmitin and 2-Elaidodipalmitin and Their Mixtures, *J. Am. Oil Chem. Soc. 53*:519–523 (1976).

[Received February 26, 1996; accepted July 16, 1996]